THE JOURNAL OF BIOLOGICAL CHEMISTRY
Vol. 280, No. 36, Issue of September 9, pp. 31936–31948, 2005
Printed in U.S.A.
© 2005 by The American Society for Biochemistry and Molecular Biology, Inc.

Mast Cell Tryptase Controls Paracellular Permeability of the Intestine

ROLE OF PROTEASE-ACTIVATED RECEPTOR 2 AND β-ARRESTINS*

Received for publication, June 10, 2005
Published, JBC Papers in Press, July 18, 2005, DOI 10.1074/jbc.M506338200

Claire Jacob‡§, Ping-Chang Yang§¶, Dalila Darmoul‡§, Silvia Amadesi‡§, Toshiyuki Saito‡§, Graeme S. Cottrell‡, Anne-Marie Coelho‡, Pamela Singh¶, Eileen F. Grady‡, Mary Perdue¶, and Nigel W. Bunnett‡‖

From the ‡Departments of Surgery and Physiology, University of California, San Francisco, California 94143 and the ¶Intestinal Disease Research Program, McMaster University, Hamilton, Ontario L8S 4L8, Canada

Tight junctions between intestinal epithelial cells prevent ingress of luminal macromolecules and bacteria and protect against inflammation and infection. During stress and inflammation, mast cells mediate increased mucosal permeability by unknown mechanisms. We hypothesized that mast cell tryptase cleaves protease-activated receptor 2 (PAR_2) on colonocytes to increase paracellular permeability. Colonocytes expressed PAR_2 mRNA and responded to PAR_2 agonists with increased $[Ca^{2+}]_i$. Supernatant from degranulated mast cells increased $[Ca^{2+}]_i$ in colonocytes, which was prevented by a tryptase inhibitor, and desensitized responses to PAR_2 agonist, suggesting PAR_2 cleavage. When applied to the basolateral surface of colonocytes, PAR_2 agonists and mast cell supernatant decreased transepithelial resistance, increased transepithelial flux of macromolecules, and induced redistribution of tight junction ZO-1 and occludin and perijunctional F-actin. When mast cells were co-cultured with colonocytes, mast cell degranulation increased paracellular permeability of colonocytes. This was prevented by a tryptase inhibitor. We determined the role of ERK1/2 and of β-arrestins, which recruit ERK1/2 to PAR_2 in endosomes and retain ERK1/2 in the cytosol, on PAR_2-mediated alterations in permeability. An ERK1/2 inhibitor abolished the effects of PAR_2 agonist on permeability and redistribution of F-actin. Down-regulation of β-arrestins with small interfering RNA inhibited PAR_2-induced activation of ERK1/2 and suppressed PAR_2-induced changes in permeability. Thus, mast cells signal to colonocytes in a paracrine manner by release of tryptase and activation of PAR_2. PAR_2 couples to β-arrestin-dependent activation of ERK1/2, which regulates reorganization of perijunctional F-actin to increase epithelial permeability. These mechanisms may explain the increased epithelial permeability of the intestine during stress and inflammation.

Tight junctions (TJs)[1] between intestinal epithelial cells are a barrier to the ingress of luminal macromolecules and bacteria into the mucosa where they induce inflammation and infection (1). TJs are composed of the transmembrane proteins occludin and claudins that interact with the zonula occludens (ZO) proteins, which bind to perijunctional actin and myosin filaments. It is important to understand the mechanisms of assembly and disassembly of TJs because they control paracellular permeability and consequently protect against mucosal inflammation. In the inflamed intestine permeability is increased, and tight junctions are lost (2–6). Moreover, cytokines, allergens, and bacterial products induce intestinal inflammation in part by causing redistribution of TJ proteins and increasing permeability (7, 8).

Mast cells control permeability of the intestinal epithelium by unknown mechanisms. Mast cells infiltrate the inflamed intestine, and the increased permeability of the intestinal epithelium during chronic stress, allergic inflammation, parasitic infection, and chemically induced inflammation is reduced in mast cell-deficient animals and by mast cell stabilizers (5, 6, 9–11). However, the mast cell products that mediate this effect and their mechanism of action are unknown.

Mast cells are replete with proteases that may induce alterations in epithelial permeability. The major protease of human mast cells is tryptase (12). Upon release, tryptase may remain active in tissues for prolonged periods as it is poorly diffusible and resistant to endogenous inhibitors (12). Antigen challenge of sensitized subjects promotes release of mast cell proteases into the intestinal lumen and vasculature, which correlates with increased permeability (13, 14). In the inflamed intestine there is also increased trypsin activity and activation of coagulation proteases (15–18). However, the effects of these proteases on permeability of the intestinal epithelium and their mechanisms of action are unknown.

Proteases can signal to cells by cleaving protease-activated receptors (PARs), a family of four G-protein-coupled receptors (reviewed in Ref. 19). PAR_2 is expressed at the apical and basolateral membrane of the intestinal epithelial cells (20).

* This work was supported by National Institutes of Health Grants DK43207, DK57840, DK39957, and DK52388. The costs of publication of this article were defrayed in part by the payment of page charges. This article must therefore be hereby marked "*advertisement*" in accordance with 18 U.S.C. Section 1734 solely to indicate this fact.

§ These authors contributed equally to this work.

‖ To whom correspondence should be addressed: University of California, San Francisco, 521 Parnassus Ave., San Francisco, CA 94143-0660. Tel.: 415-476-0489; Fax: 415-476-0936; E-mail: nigelb@itsa.ucsf.edu.

[1] The abbreviations used are: TJ, tight junction; siRNA, small interfering RNA; PAR_2, protease-activated receptor 2; ZO, zonula occludens; ERK1/2, extracellular signal-regulated kinases 1/2; βARR, β-arrestin; SBTI, soybean trypsin inhibitor; FCS, fetal calf serum; PBS, phosphate-buffered saline; BSA, bovine serum albumin; PVDF, polyvinylidene difluoride; RT, reverse transcription; TER, transepithelial resistance; AP, activating peptide; RP, reverse peptide; HRP, horseradish peroxidase; MEK, mitogen-activated protein kinase/ERK kinase; CHMC, cultured human mast cells; DAPI, 4,6-diamidino-2-phenylindole; HBSS, Hanks' balanced salt solution.

This paper is available on line at http://www.jbc.org

This is an Open Access article under the CC BY license.

Tryptase, trypsins, and coagulation factors VIIa and Xa cleave PAR_2 within the extracellular N terminus at Ser-Lys-Gly-Arg-Ser^{34}↓Leu-Ile-Gly-Lys-Val (human, ↓ = cleavage site) to expose a tethered ligand domain (SLIGKV) that binds to and activates the cleaved receptor (21–25). Injection of trypsin and PAR_2-activating peptide (AP, corresponding to the tethered ligand) into the intestinal lumen increases epithelial permeability and promotes infiltration of bacteria (26–28). However, the mechanisms by which PAR_2 activation couples to assembly of TJs and regulates interactions of TJ proteins with the cytoskeleton are unknown. In enterocytes, PAR_2 interacts with the multi-adaptor protein β-arrestin (βARR), which mediates receptor endocytosis and recruits activated extracellular signal-regulated kinases 1/2 (ERK1/2) to endosomes (29). Cytosolically retained ERK1/2 may regulate the cytoskeleton to control paracellular permeability (30, 31).

We hypothesized that mast cells signal to colonocytes by release of tryptase and activation of PAR_2, and that PAR_2 couples to ERK1/2 by a βARR-dependent mechanism to regulate TJ assembly, perijunctional filamentous actin (F-actin), and paracellular permeability. Our goals were as follows: 1) to examine expression of PAR_2 by colonocytes; 2) to investigate the effects of PAR_2 activation on assembly of TJs and permeability; 3) to determine whether mast cells signal to colonocytes to increase permeability by release of tryptase and activation of PAR_2; and 4) to investigate the role of ERK1/2 and βARR in this process.

EXPERIMENTAL PROCEDURES

PAR_2 Agonists and Protease Inhibitors—Sources of pancreatic trypsin, AP (human SLIGKV-NH_2 or rat/mouse SLIGRL-NH_2), and the inactive reverse peptide (RP) (VKGILS-NH_2 or LRGILS-NH_2 control) have been described (32). Identical results were obtained with both APs. The tryptase inhibitors BABIM (33) and RWJ337842 (CAS number 607392-92-7) (34) were from R. Tidwell (University of North Carolina) and P. Andrade-Gordon (R. W. Johnson Pharmaceutical Research Institute), respectively. Soybean trypsin inhibitor (SBTI) was from Sigma.

Antibodies—Rabbit antibody to human IgE was from Bethyl Laboratories (Montgomery, TX); mouse antibody to human tryptase was from Serotec Inc. (Raleigh, NC); rabbit ZO-1, mouse occludin, and mouse claudin1 antibodies were from Zymed Laboratories Inc.; mouse E-cadherin antibody was from Upstate Biotechnology, Inc. (Lake Placid, NY). Antibodies to phosphorylated ERK1/2 (pERK1/2) and ERK2 were from Santa Cruz Biotechnology (Santa Cruz, CA). βARR1 antibody was from BD Transduction Laboratories, and βARR2 antibody was from R. Lefkowitz (Duke University). Antibody to γ-tubulin was from Convince (Berkeley, CA). Mouse primary antibody isotype control and chromatographically purified rabbit IgG were from Zymed Laboratories Inc., and rabbit IgG isotype control was from Bethyl Laboratories. Fluorescein isothiocyanate- and peroxidase-conjugated goat anti-rabbit and anti-mouse IgG were from Jackson ImmunoResearch (West Grove, PA). Texas Red-, Alexa 488-, and phycoerythrin-conjugated goat anti-rabbit and anti-mouse IgG were from Molecular Probes (Eugene, OR).

Colonic Epithelial Cells—T84 colonic epithelial cells (American Type Culture Collection, Manassas, VA) were cultured in Dulbecco's modified Eagle's medium/F-12 with 5% FCS, 14 mM sodium bicarbonate, 15 mM HEPES, 100 units/ml penicillin, and 100 μg/ml streptomycin (5% CO_2, 37 °C). NCM460 cells (R. Benya, University of Illinois), a nontransformed human colonocyte line (35), were cultured in Ham's F-12 medium with 20% FCS, 0.5 units/ml insulin-transferrin, 0.4 μg/ml hydrocortisone, and 0.58 μg/ml glutamine (5% CO_2, 37 °C). T84 and NCM460 cells were plated on plastic for RT-PCR and ERK1/2 assays and on glass coverslips for measurement of $[Ca^{2+}]_i$. T84 cells were plated on transwell polycarbonate filters (0.4 μm pore, 4.7 cm^2, 0.5–1.0 × 10^6 cells/well) for study of permeability and redistribution of junctional proteins (7). Studies commenced when transepithelial resistance (TER) exceeded 1,000 $\Omega \cdot cm^{-2}$, determined using Millicell ERS apparatus (Millipore, Bedford, MA). When used, T84 cells were treated with the 10 μM MEK inhibitor UO126 (Calbiochem) for 30 min prior to adding AP or RP, and TER and F-actin localizations were assessed after 24 h.

Mast Cells—Cultured human mast cells (CHMC, Rigel Pharmaceuticals, South San Francisco, CA) were derived from CD34+ precursor cells from umbilical cord blood. Cells were cultured for 5 days in StemPro medium (Invitrogen) containing 200 ng/ml stem cell factor, 20 ng/ml flt3 ligand, 200 ng/ml interleukin 6, and 100 ng/ml IgE (all from Cortex Biochem. Inc., San Leandro, CA) to induce differentiation into mucosal type mast cells containing tryptase and not chymase. The human mast cell line HMC1 (J. H. Butterfield, Mayo Clinic, Rochester, MN (36)) was cultured in Iscove's modified Dulbecco's medium containing 10% iron-supplemented FCS, 1.2 mM α-thioglycerol, 100 units/ml penicillin, and 100 μg/ml streptomycin (5% CO_2, 37 °C). To induce degranulation, CHMC (5 × 10^6 cells/ml HBSS, 0.1% BSA, 20 mM HEPES, 25 μg/ml heparin, pH 7.4) were challenged with rabbit IgE antibody (1:1,000, 30 min, 37 °C) or vehicle (control). HMC1 (10^6 cells/ml Dulbecco's modified Eagle's medium) were challenged with compound 48/80 (5 μg/ml, 15 min, 37 °C) to induce degranulation. After treatments, CHMC and HMC1 were pelleted (14,000 × *g*, 5 min, 4 °C), and supernatants were assayed for tryptase and effects on $[Ca^{2+}]_i$ and permeability of colonocytes.

Co-culture of T84 and HMC1 Cells—T84 cells (10^6 cells/well) were cultured on filters until confluent. HMC1 cells were added to the basal compartment (10^6 cells in 1.5 ml). Cells were co-cultured in Iscove's modified Dulbecco's medium. To degranulate mast cells, compound 48/80 (5 μg/ml) was added to the basal compartment. Permeability of the T84 monolayers was determined after 24 h.

RT-PCR—Total RNA from T84 and NCM460 cells was reverse-transcribed. PCRs used primers specific for PAR_2 (forward, 5′-ccctttgtatgtcgtgaagcagac-3′; reverse, 5′-ttcctggagtgtttctttgaggtg-3′), trypsinogens (forward, 5′-gccaagcttcgcgtgtccaccatctgtgtcg-3′; reverse, 5′-cagcggccgcttagctgttggcagctatggtg-3′), βARR1 (forward, 5′-ggacaagaagcccctgacgcg-3′; reverse, 5′-agcctcttccatggcaacagg-3′), and βARR2 (forward, 5′-tcaactcgaacaagatgacca-3′; reverse 5′-gtggcatagttggtatcaaat-3′). Reverse transcriptase was omitted from controls. PCR products were separated by electrophoresis and sequenced.

Tryptase Assay—Samples were incubated with 200 μl of 50 mM Tris/HCl, pH 7.6, 120 mM NaCl, 20 μg/ml heparin containing 0.5 mM tosyl-Gly-Pro-Arg-*p*-nitroanilide (Sigma) for 15 min at 37 °C. Absorbance was measured at 405 nm to assess cleavage. Inhibitors were preincubated with samples for 15 min on ice before assay. Results are expressed as nanomoles of cleaved substrate/min/10^6 cells.

Measurement of $[Ca^{2+}]_i$—T84 and NCM460 cells were incubated in HBSS with 0.1% BSA, 20 mM HEPES, pH 7.4, and 2.5–5 μM Fura-2AM (Molecular Probes, Eugene, OR) for 30–45 min at 37 °C. Coverslips were mounted in an open chamber (500 μl volume) in HBSS with 0.1% BSA, 20 mM HEPES, pH 7.4, at 37 °C, and fluorescence of individual cells was measured at 340 and 380 nm excitation and 510 nm emission (22). A Fura-2 calcium imaging calibration kit (Molecular Probes) was used to calculate $[Ca^{2+}]_i$ according to the manufacturer's directions. A standard curve was generated (0.017–39.8 μM) and used to convert the emission ratio at 340/380 nm excitation to estimate the free $[Ca^{2+}]_i$. AP or proteases were added directly to the chamber in a volume of 50 μl, and maximal increases in $[Ca^{2+}]_i$ were determined. In assays of mast cell products, the supernatant was obtained from 5 × 10^6 CHMC or HMC1, and 50 μl was added to the chamber to a final volume of 500 μl. When used, cells were preincubated with RWJ337842 (10 μM) for 2 min. To assess the contribution of extracellular Ca^{2+} ions to changes in $[Ca^{2+}]_i$, cells were incubated in Ca^{2+}-free HBSS with 0.1% BSA, 20 mM HEPES, pH 7.4. For concentration-response analyses, cells were exposed to a single concentration of agonists and then 5 μM ionomycin. Results were normalized and are expressed as percent responses to 5 μM ionomycin. The EC_{50} was calculated by using Origin Microcal software (Northampton, MA). For desensitization experiments, cells were preincubated with proteases or vehicle (control) for 2–5 min and then challenged with AP, without an intervening wash. Observations were repeated in >4 separate experiments.

TER and Paracellular Flux of Macromolecules—Test substances were added to the apical or basal compartments of transwell with confluent T84 cells on filters. TER was determined as described at 0–48 h. Results are expressed as $\Omega \cdot cm^{-2}$ and are normalized as percentage of base-line values. To measure paracellular flux of macromolecules, horseradish peroxidase (HRP, 44 kDa, type II, Sigma, 0.01 mM) was added to the apical compartment at 24 h. After 2 h, samples were obtained from medium in the apical and basolateral compartments and assayed for HRP using a kinetic enzymatic assay as described (9, 10). HRP flux is expressed as percentage of apically added HRP recovered in basolateral compartment over 2 h. Measurements of TER and HRP flux were made from four wells per experiment, and experiments were repeated four times.

Immunofluorescence—T84 cells grown to confluence on filters were fixed in 4% paraformaldehyde in 100 mM PBS, pH 7.4, for 20 min at 4 °C. Cells were washed and incubated in PBS with 5% normal goat

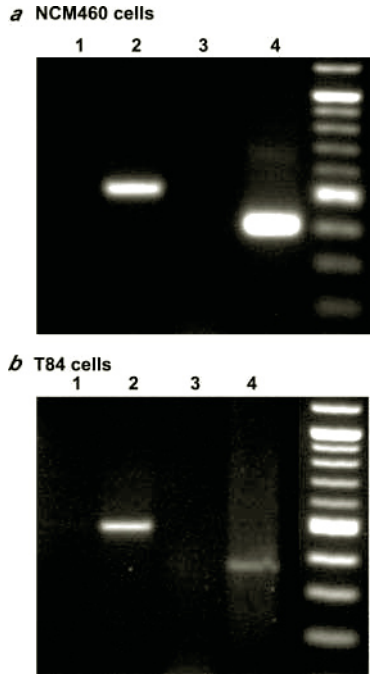

FIG. 1. **Expression of mRNA encoding PAR$_2$ and trypsinogen IV by colonocytes.** Amplification of colonocyte PAR$_2$ (*lane 2*) and trypsinogen IV (*lane 4*) by RT-PCR in NCM460 cells (*a*) T84 cells (*b*). *Lanes 1* and *3* are controls (no RT). The products were identified by sequencing.

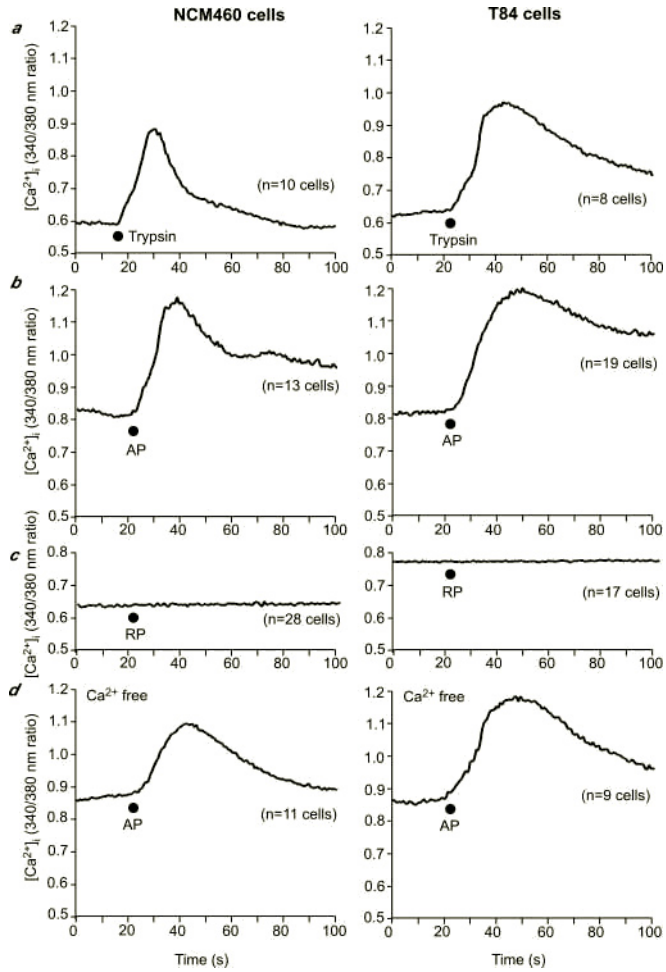

FIG. 2. **PAR$_2$-mediated mobilization of $[Ca^{2+}]_i$ in colonocytes.** Effects of trypsin (10 nM) (*a*), AP (100 μM) (*b*), and RP (100 μM) (*c*) in the presence of extracellular Ca^{2+} ions, and effects of AP (100 μM) (*d*) in the absence of extracellular Ca^{2+} ions on $[Ca^{2+}]_i$ in NCM460 (*left panels*) and T84 cells (*right panels*). The results are expressed as 340/380 nm ratio. Each trace is a mean of traces from the indicated number of cells ($n > 4$ experiments). Note that the response to trypsin and AP consists of a peak and a plateau response, both of which are diminished in the Ca^{2+}-free buffer.

serum, 0.3% Triton X-100 with primary antibodies to junctional proteins: rabbit ZO-1, mouse occludin, and mouse claudin1 (1:50–200, overnight, 4 °C). Filters were washed and incubated with fluorescein isothiocyanate-conjugated goat anti-IgG or anti-mouse (1:200, 2 h, room temperature). To detect F-actin, fixed, permeabilized cells were incubated with Texas Red-X-phalloidin (5 units/ml, Molecular Probes) for 20 min at room temperature. Cells were mounted in Prolong with DAPI (Molecular Probes). To localize IgE receptor and tryptase in CHMC, fixed and permeabilized cells were incubated with rabbit anti-human IgE (2 μg/ml) and mouse anti-human tryptase (2 μg/ml) antibodies (overnight, 4 °C), washed, incubated with Texas Red- and Alexa 488-conjugated goat anti-rabbit and mouse IgG (1:100, 2 h, room temperature), and mounted. In control experiments, the primary antibodies were replaced with isotype control antibodies at the same dilutions.

Microscopy—For confocal microscopy, specimens were observed using a Zeiss Axiovert microscope with a Bio-Rad MRC1000 confocal microscope using Zeiss Fluar ×20 (NA 1.0), Plan Apo ×40 (NA 1.4), ×100 (NA 1.3) objectives (29). For z projections, 125–300 line sections were taken at 0.2-μm intervals to enable observation of the apical and basal membranes of T84 cells on filters. For epifluorescence microscopy, specimens were observed using a Zeiss Axioplan microscope with a Spot digital camera (Diagnostic Instruments, McHenry, IL). Images were processed to adjust contrast and brightness using Adobe Photoshop 7.0 (Adobe Systems, Mountain View, CA).

Flow Cytometry—CHMC, which had been cultured with 100 ng/ml IgE for 5 days, were suspended in 100 mM PBS, pH 7.4, containing 2% fetal bovine serum (0.5×10^6 cells/ml). Cells were incubated with rabbit anti-human IgE antibody (5 μg/ml) or rabbit IgG isotype control (5 μg/ml) for 15 min at 4 °C. Cells were washed and incubated with phycoerythrin-conjugated goat anti-rabbit IgG (2 μg/ml) for 15 min at 4 °C. Cells were washed and suspended in 1 ml of PBS/fetal bovine serum. Cells were analyzed with a FACSCalibur flow cytometer (BD Biosciences). Fluorophores were excited at 488 nm, and emission was collected at 575/25 nm for phycoerythrin.

Cellular Fractionation and Western Blotting—T84 cells were lysed in 1% Triton X-100, 100 mM NaCl, 10 mM HEPES, pH 7.6, 2 mM EDTA with protease inhibitors (Roche Applied Science) and passed 10 times through a 21-gauge needle. Lysates were centrifuged ($15{,}000 \times g$, 30 min, 4 °C), and the supernatant formed the Triton-soluble or cytosolic fraction. The pellet was ultrasonicated in Triton buffer containing 1% SDS and cleared ($15{,}000 \times g$, 5 min, 4 °C) to give the Triton-insoluble or TJ fraction. Samples (5–20 μg of protein determined by Bradford method) were fractionated on 7–15% SDS-polyacrylamide gel and transferred to PVDF membranes (Millipore, Bedford, MA). Membranes were blocked in Tris-buffered saline, 0.1% Tween 20, 5% nonfat dry milk for 1 h, and blots were incubated with primary antibodies for 2 h at room temperature: Z-O1, occludin, claudin-1, and E-cadherin (1:100–1:200). Membranes were washed and incubated with goat anti-mouse or -rabbit IgG conjugated to peroxidase (1 h, room temperature), and proteins were detected by chemiluminescence (ECL Plus, Amersham Biosciences). Experiments were repeated four times.

ERK1/2 Assays—T84 cells were serum-deprived for 12–16 h. Cells were lysed with 100 μl of RIPA (10 mM Tris/HCl, 200 mM NaCl, 50 mM NaF, 1 mM $NaVO_4$, 0.5% deoxycholate, 0.1% SDS, 1% Nonidet P-40, 1 mM EDTA, pH 7.4) with protease inhibitors. Samples (5–20 μg of protein determined by Bradford method) were fractionated by 10% Tris-glycine SDS-polyacrylamide gels and transferred to PVDF membranes. Membranes were incubated with antibody to pERK1/2 (1:5,000 overnight, 4 °C) (29). Membranes were stripped and reblotted for ERK2 (1:5,000 overnight, 4 °C). Signals were detected using peroxidase-conjugated secondary antibodies and chemiluminescence. Experiments were repeated four times.

βARR siRNA—siRNA duplexes of 21-nucleotide sense and 21-nucleotide antisense strands with 2-nucleotide 3′-dTdT overhangs were designed to target rat βARR1 (GenBank™ accession number NM_012910) and βARR2 (GenBank™ accession number NM_012911.1) by searching for the motif AA(N19) (where N indicates any nucleotide) and selecting unique sequences (determined by blast of NCBI data base) with ~50% G/C content (Dharmacon Research, Lafayette, CO). Chosen sequences were βARR1 5′-gagcgacucaucaagaagcdTdT-3′ (304–322 from start codon)

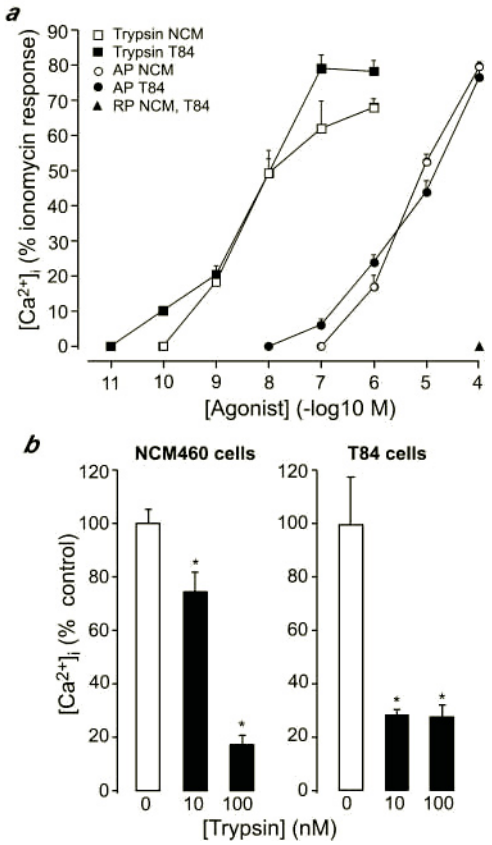

FIG. 3. **PAR_2-mediated mobilization of $[Ca^{2+}]_i$ in colonocytes.** *a,* effects of graded concentrations of AP and trypsin on $[Ca^{2+}]_i$ of NCM460 and T84 cells, expressed as % response to ionomycin. Each point is a mean of the responses of 14–25 cells, $n > 4$ experiments. *b,* effects of preincubation with 0 (vehicle), 10, or 100 nM trypsin for 5 min on Ca^{2+} response to 100 μM AP. Results are expressed as a percentage of the control response of vehicle-treated cells. Each point is a mean of the responses of 10–30 cells ($n > 4$ experiments). *, $p < 0.05$ compared with vehicle control.

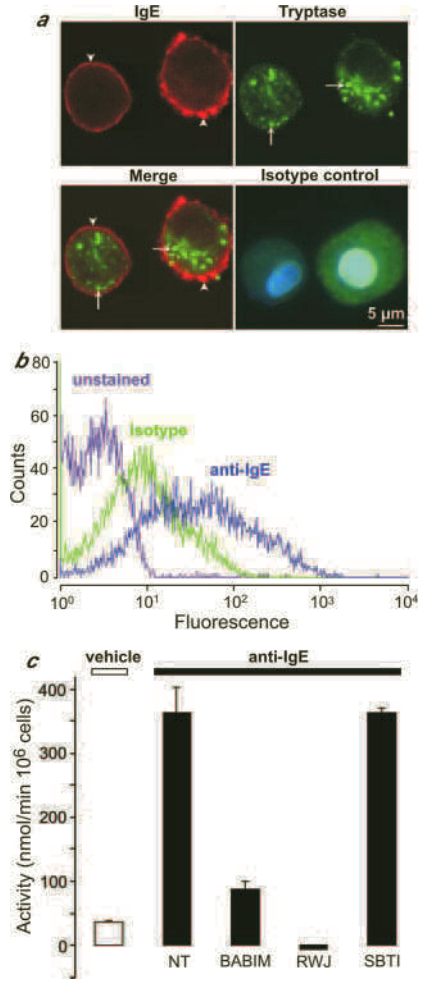

FIG. 4. **Characterization of CHMC.** *a,* localization of IgE (*red*) and tryptase (*green*) in CHMC by immunofluorescence and confocal microscopy. *Arrowheads* indicate surface-bound IgE, and *arrows* show tryptase in granules. There was minimal signal other than autofluorescence when the primary antibodies to tryptase and IgE were replaced with isotype control antibodies. The nucleus is stained with DAPI. Representative images of $n > 4$ experiments are shown. *b,* detection of surface IgE by flow cytometry, showing specific binding of anti-IgE compared with isotype control antibody and unstained cells. Representative images of $n > 4$ experiments are shown. *c,* enzymatic assay of tryptase activity in supernatant collected from CHMC incubated with vehicle or anti-IgE to induce degranulation. The tryptase inhibitors BABIM and RWJ337842 (RWJ) abolished activity, whereas SBTI had no effect ($n > 4$ experiments).

and βARR2 5′-cucaagcacgaagacaccadTdT-3′ (880–898 from start codon), and control siRNA 5′-aacgaagcaacuaagcucgdTdT-3′ did not target any gene. T84 cells (30–50% confluence for βARR Western blotting and ERK1/2 assays and TER >1,000 $\Omega \cdot cm^{-2}$ for permeability assays) were transfected with siRNA (5 μl of 20 μM stock added apically) using Oligofectamine (Invitrogen) according to the manufacturer's directions. For βARR Western blotting, cells were lysed at various times after transfection with 100 μl of RIPA (10 mM Tris/HCl, 200 mM NaCl, 50 mM NaF, 1 mM $NaVO_4$, 0.5% deoxycholate, 0.1% SDS, 1% Nonidet P-40, 1 mM EDTA, pH 7.4) with protease inhibitors. Samples (5–20 μg of protein determined by Bradford method) were fractionated by 10% Tris-glycine SDS-polyacrylamide gels and transferred to PVDF membranes. βARR1 and -2 were detected by Western blotting of whole cell lysates using antibodies to βARR1 (1:300, overnight, 4 °C) or βARR2 (1:2,500, overnight, 4 °C). Membranes were stripped and re-blotted for γ-tubulin (1:3,000, overnight, 4 °C). Signals were detected using peroxidase-conjugated secondary antibodies and chemiluminescence. Experiments were repeated 3–4 times. The effects of AP on activation of ERK1/2 and on TER and HRP flux were examined 3–4 days after transfection.

Densitometry—Western blot signals were quantified using Scion Image software (Scion Corporation, Frederick, MD), and densitometry data from independent experiments were averaged for statistical analysis.

Statistics—Results are expressed as mean ± S.E. and are compared by analysis of variance and Student-Newman-Keul's test, with $p < 0.05$ considered significant.

RESULTS

Characterization of PAR_2 Expression by Colonocytes—We examined expression of PAR_2 and the PAR_2 agonist trypsinogen IV (24) in NCM460 and T84 cells using RT-PCR. Transcripts with the predicted size for PAR_2 (525 bp) were detected in both NCM460 cells (Fig. 1*a*, *lane 2*) and T84 cells (Fig. 1*b*, *lane 2*). In both cases the products were sequenced to confirm identity as PAR_2 transcripts. Primers designed to amplify all human trypsinogens (I, II, mesotrypsinogen, and IV) amplified products of the predicted size (400 bp) in NCM460 cells (Fig. 1*a*, *lane 4*) and T84 cells (Fig. 1*b*, *lane 4*). The products were identified as trypsinogen IV by sequencing. There were no signals in control experiments where reverse transcriptase was omitted.

To determine whether colonocytes express functional PAR_2, we measured changes in $[Ca^{2+}]_i$ in response to PAR_2 agonists. The basal $[Ca^{2+}]_i$ was 4.63 ± 0.80 nM in NCM460 cells ($n = 23$ cells) and 5.32 ± 0.95 nM in T84 cells ($n = 27$ cells, $n > 4$ experiments). Trypsin (10 nM) increased $[Ca^{2+}]_i$ in NCM460 cells by 3.10 ± 0.63 nM ($n = 10$ cells) and T84 cells by 3.72 ± 1.11 nM ($n = 8$ cells) above basal values (Fig. 2*a*). AP (100 μM) increased $[Ca^{2+}]_i$ in NCM460 cells by 4.31 ± 0.61 nM ($n = 13$ cells) and T84 cells by 4.49 ± 0.52 nM ($n = 19$ cells) above basal values (Fig. 2*b*). RP (100 μM) had no effect on

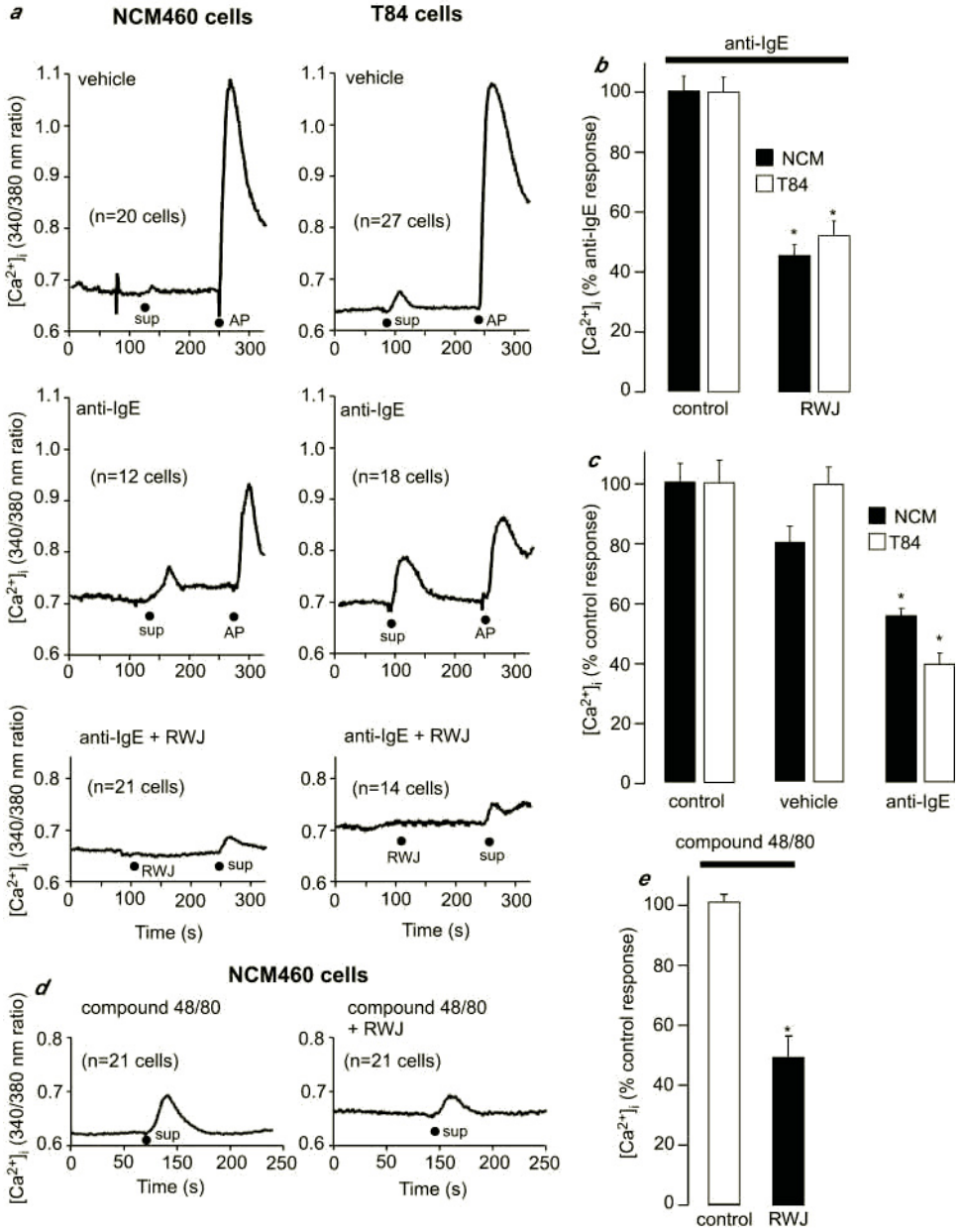

FIG. 5. **Mast cell signaling to colonocytes.** *a,* effects of supernatant (*sup*) from CHMC on $[Ca^{2+}]_i$ in NCM460 cells (*left*) and T84 cells (*right*). *Upper panels* show that supernatant from undegranulated CHMC (vehicle-treated) caused a small increase in $[Ca^{2+}]_i$ and that cells responded normally to AP (100 μM). *Middle panels* show that supernatant from degranulated CHMC (anti-IgE-treated) caused a large increase in $[Ca^{2+}]_i$ and induced desensitization of responses to AP. *Lower panels* show that addition of the tryptase inhibitor RWJ337842 (*RWJ*) markedly inhibited the stimulatory effects of supernatant from degranulated CHMC. The results are expressed as 340/380 nm ratio. Each trace is a mean of traces from the indicated number of cells ($n > 4$ experiments). *b,* effects of RWJ337842 on $[Ca^{2+}]_i$ in colonocytes challenged with supernatant from degranulated CHMC. Results are expressed as a percentage of the response obtained in nontreated cells (control, 100%) ($n = 4$ experiments). Note that RWJ337842 inhibited the action of supernatant by ~50%. *c,* desensitization of AP-induced increase in $[Ca^{2+}]_i$ in colonocytes. Results are expressed as a percentage of the response obtained in nontreated cells (control, 100%) ($n = 4$ experiments). Note that preincubation of colonocytes with supernatant from degranulated CHMC desensitized AP-induced $[Ca^{2+}]_i$ by ~50%, whereas preincubation with supernatant from undegranulated cells had no effect. *d,* effects of supernatant from degranulated HMC1 (compound 48/80-treated) on $[Ca^{2+}]_i$ in NCM460 in the absence (*left*) and in the presence (*right*) of RWJ337842. Each trace is a mean of traces from the indicated number of cells. *e,* effects of RWJ337842 on $[Ca^{2+}]_i$ of colonocytes challenged with supernatant from degranulated HMC1. Results are expressed as a percentage of the response obtained in nontreated cells (control, 100%) ($n = 4$ experiments). Note that RWJ337842 inhibited the effect of supernatant by ~50%. *, $p < 0.05$ compared with control.

$[Ca^{2+}]_i$ in NCM460 or T84 cells, confirming specificity of AP (Fig. 2*c*).

In both cell lines there was a biphasic change in $[Ca^{2+}]_i$ in response to PAR_2 agonists, with an initial rapid increase followed by a sustained plateau. This plateau was more prominent in T84 cells than NCM460 cells. To determine the contribution of extracellular Ca^{2+} to this biphasic response, experiments were repeated in the Ca^{2+}-free buffer. In the absence of extracellular Ca^{2+}, both phases of the response to PAR_2 agonists were diminished in NCM460 and T84 cells (Fig. 2*d*). Thus, in NCM460 cells treated with AP (100 μM), the maximal response was diminished by 41.7%, and the sustained response (measured at 50 s after AP) was reduced by 63.2% by removal of extracellular Ca^{2+} ($n = 11$ cells). In T84 cells treated with AP (100 μM), the maximal response was diminished by 16.2%, and the sustained response (measured at 50 s after challenge) was reduced by 33.3% by removal of extracellular Ca^{2+} ($n = 9$ cells). Similar results were obtained in

trypsin-stimulated cells (not shown). Thus, PAR_2 agonists signal to colonocytes to induce a rapid increase followed by a sustained elevation in $[Ca^{2+}]_i$, which are both diminished but not abolished by removal of Ca^{2+} ions from the extracellular fluid. These results suggest that both phases depend in part on mobilization of Ca^{2+} ions from intracellular stores and in part on influx of extracellular Ca^{2+} ions.

To characterize further the receptors responsible for trypsin- and AP-induced increases in $[Ca^{2+}]_i$ in colonocytes, we determined the potencies and efficacies of the responses. Trypsin increased $[Ca^{2+}]_i$ with an EC_{50} of 3.24 ± 0.03 nM in NCM460 cells and 5.13 ± 0.10 nM in T84 cells, and AP increased $[Ca^{2+}]_i$ with an EC_{50} of 6.17 ± 1.18 μM in NCM460 cells and 4.90 ± 1.20 μM in T84 cells (n = 14–25 cells per data point, $n > 4$ experiments) (Fig. 3*a*). The responses to the maximal tested concentration of AP (100 μM) were the same in NCM460 and T84 cells, although the responses to the highest concentrations of trypsin (1 μM) were higher in T84 cells.

Because trypsin may signal by cleaving receptors other than PAR_2, we determined whether preincubation with trypsin desensitized responses to AP. Cells were incubated with 10 or 100 nM trypsin or vehicle (control) for 5 min and challenged with 100 μM AP. Preincubation with trypsin markedly desensitized responses to AP. When compared with control cells, responses to AP in NCM460 were reduced by 25 and 83%, after trypsin 10 and 100 nM, respectively. The response to AP in T84 was reduced by >70% after both concentrations or trypsin (Fig. 3*b*).

Together, these results indicate that colonocytes express PAR_2 and respond to the PAR_2 agonists AP and trypsin, and trypsin increases $[Ca^{2+}]_i$ by cleaving PAR_2.

Mast Cells Signal to Colonocytes by Tryptase and PAR$_2$—Tryptase cleaves and activates PAR_2 on many cell types, including intestinal epithelial cells (19, 21, 22).[2] However, it is not known if mast cells signal to colonocytes by release of tryptase and activation of PAR_2 or by other mechanisms. Therefore, we determined whether mast cells release tryptase upon stimulation and whether a supernatant from degranulated mast cells signals to colonocytes by tryptase activation of PAR_2.

The mast cell line HMC1 is thoroughly characterized and contains and releases tryptase upon stimulation (*e.g.* with compound 48/80) (22, 36). We also characterized CHMC and determined whether they contain tryptase and release the protease after appropriate stimulation. When CHMC were cultured with IgE, immunoreactive IgE was detected at the plasma membrane by immunofluorescence and confocal microscopy (Fig. 4*a*, *arrowheads*). Immunoreactive tryptase was detected in granules that were densely packed in the cytosol (Fig. 4*a*, *arrows*). There was no staining in cells incubated with isotype control antibodies (Fig. 4*a*). The surface expression of IgE receptor was also confirmed by flow cytometry, which revealed specific surface binding of anti-IgE but not of isotype control antibody (Fig. 4*b*). Thus, CHMC bind IgE and therefore express IgE receptors and also contain tryptase in secretory granules. We cross-linked IgE receptors by incubating CHMC with IgE followed by IgE antibody (anti-IgE), and we measured enzymatic activity in the supernatant from degranulated cells using the tryptase substrate tosyl-Gly-Pro-Arg-*p*-nitroanilide. Incubation of CHMC with anti-IgE for 30 min induced an ~10-fold increase in enzymatic activity in the supernatant over vehicle-treated cells (Fig. 4*c*). This activity was strongly suppressed by the tryptase inhibitors BABIM (10 μM) and RWJ337842 (10 μM) but was unaffected by SBTI (50 μg/ml), which does not inhibit tryptase but does inhibit trypsins that can also cleave this substrate. Thus, CHMC, like HMC1, contain and release tryptase.

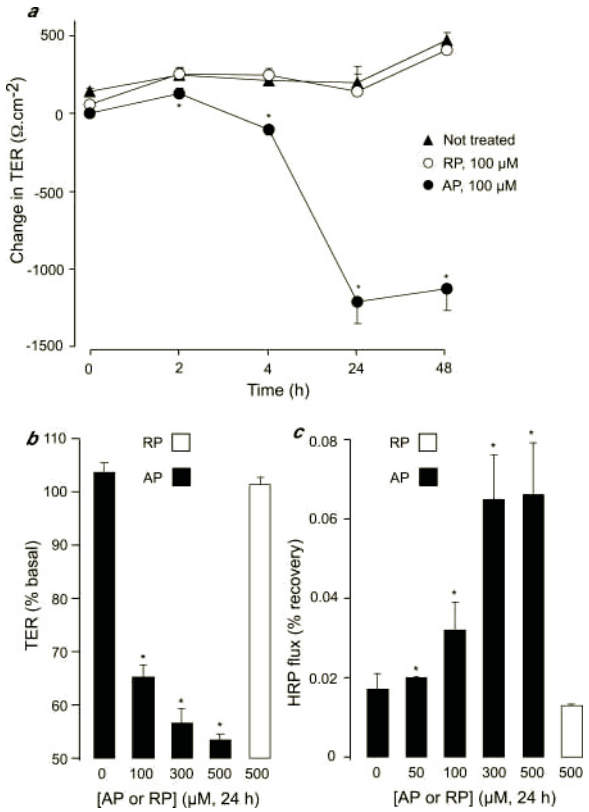

FIG. 6. **Effects of PAR$_2$ agonists on paracellular permeability.** AP or RP were applied to the basolateral membrane of T84 cells. *a,* time course of effects of AP and RP on TER, expressed as $\Omega \cdot cm^{-2}$. *b,* concentration-response analysis of the effects of AP and RP on TER measured at 24 h, expressed as percent of basal values at 0 min. *c,* concentration-response analysis of the effects of AP and RP on HRP flux, expressed as percentage of apically added HRP recovered into the basolateral compartment from 24 to 26 h. *, $p < 0.05$ compared with RP. Quadruplicate observations in n = 4 experiments.

We also determined whether supernatant from degranulated mast cells increased $[Ca^{2+}]_i$ in colonocytes by tryptase activation of PAR_2. Supernatant from undegranulated CHMC (vehicle-treated) had a small effect on $[Ca^{2+}]_i$ in NCM460 and T84 cells, but cells still responded in the expected manner to AP (Fig. 5*a*, *upper panels*). Supernatant from degranulated CHMC (anti-IgE-treated) induced a rapid increase in $[Ca^{2+}]_i$ in NCM460 and T84 cells (Fig. 5*a*, *middle panels*). Addition of the tryptase inhibitor RWJ337842 (10 μM, injected 2 min before supernatant) markedly inhibited the effects of supernatant from degranulated CHMC by ~50% in both NCM460 and T84 cells (Fig. 5, *a*, *lower panels,* and *b*). The effects of BABIM on this response could not be examined because BABIM or a metabolite interfered with measurement of $[Ca^{2+}]_i$ (results not shown). These results suggest that tryptase is a major component of the supernatant obtained from degranulated mast cells that signals to colonocytes. To determine whether the effect of supernatant from degranulated CHMC on $[Ca^{2+}]_i$ was because of activation of PAR_2, we assessed desensitization of responses to AP. Cells were either untreated (control), preincubated with supernatant from undegranulated CHMC, or degranulated CHMC for 2 min and then challenged with AP (100 μM). Preincubation with supernatant from undegranulated CHMC did not affect AP-induced increases in $[Ca^{2+}]_i$ in colonocytes (Fig. 5, *a*, *upper panels,* and *c*), whereas supernatant from degranulated CHMC desensitized the response to AP by 45% in NCM460 and 61% in T84 cells (Fig. 5, *a*, *middle panels,* and *c*).

[2] N. W. Bunnett, unpublished data.

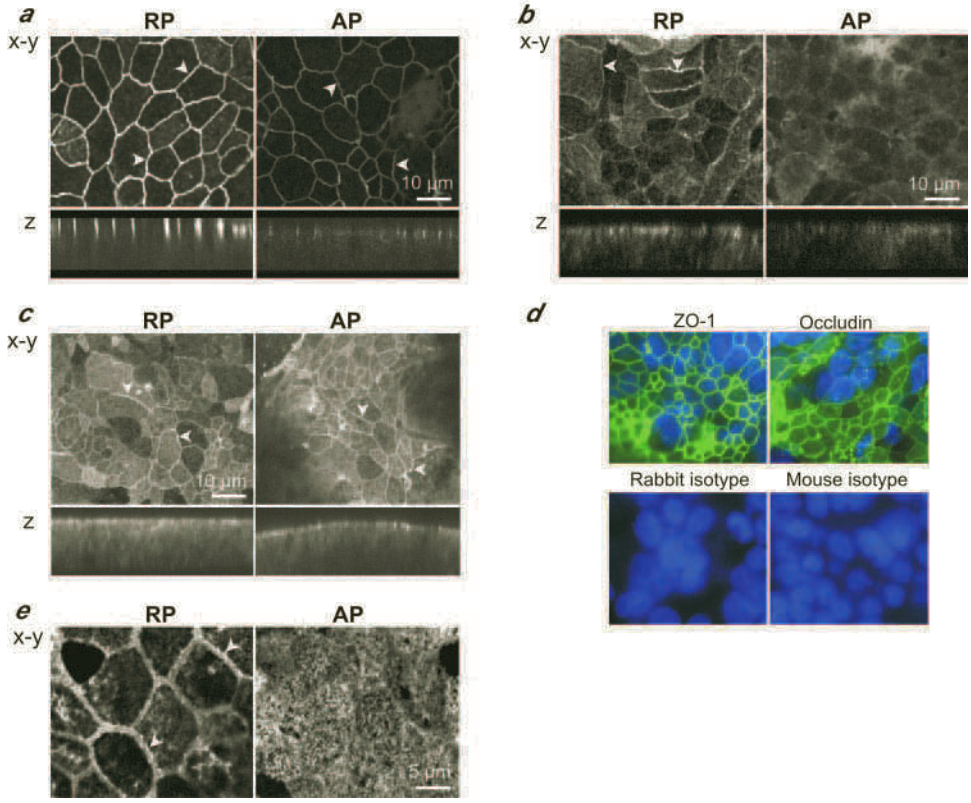

FIG. 7. **PAR$_2$-induced redistribution of TJ proteins and F-actin detected by microscopy.** AP or RP (100 μM) was applied to T84 cells for 24 h. *a,* confocal images showing localization of immunoreactive ZO-1 to tight junctions in the apical region of cells treated with RP that was diminished in cells treated with AP (*arrowheads*). The z projection shows redistribution of a portion of ZO-1 from the tight junctional region. *b,* confocal images showing localization of immunoreactive occludin to apical tight junctions in RP-treated cells, with some redistribution from the tight junctions after incubation with AP. *c,* confocal images showing localization of immunoreactive claudin-1 to apical tight junctions in RP- and AP-treated cells. *d,* epifluorescence images of T84 cells. The *upper panels* show localization of ZO-1 and occludin to apical tight junctions (*green*). The *lower panels* are controls in which primary antibodies were replaced with isotype control antibodies of the same species. Nuclei are stained with DAPI. *e,* confocal images showing localization of F-actin with Texas Red phalloidin in a perijunctional region in RP-treated cells (*arrowheads*) and redistribution after exposure to AP. Representative images of $n > 4$ experiments.

These results suggest that the effects of the supernatant on $[Ca^{2+}]_i$ are mediated in part by activation of PAR$_2$. We similarly determined whether the stable mast cell line HMC1 could signal to colonocytes through release of tryptase and activation of PAR$_2$. Compound 48/80 degranulated HMC1 to release tryptase-like activity that was inhibited by RWJ337842 and BABIM but not SBTI (not shown). Also, supernatant from degranulated HMC1 increased $[Ca^{2+}]_i$ in NCM460 cells (Fig. 5*d*), and RWJ337842 inhibited this effect by >50% (Fig. 5*e*).

Together, these results suggest that mast cells can signal to colonocytes by release of tryptase and activation of PAR$_2$. In subsequent experiments we studied HMC1, as this is a stable mast cell line, and T84 cells that maintain a high TER and are commonly used as a model to study paracellular permeability (7).

PAR$_2$ Activation Increases Paracellular Permeability—To assess the effects of PAR$_2$ activation on permeability of T84 cells, we measured TER and transepithelial flux of HRP. AP and trypsin applied to the basolateral membrane induced a time-dependent decrease in TER within 2 h that was maximal at 24 h (100 μM AP, 55.2 ± 2.7% basal; 10 nM trypsin, 61.3 ± 3.5% basal) and sustained for 48 h (Fig. 6*a* for AP, trypsin not shown). RP (Fig. 6*a*) and heat-inactivated trypsin (not shown) were ineffective. AP and trypsin applied to the apical membrane of T84 cells induced a smaller decline in TER (24 h: 100 μM AP, 78.3 ± 2.8% basal; 10 nM trypsin, 76.0 ± 3.5% basal). Thus, in subsequent experiments agonists were applied to the basolateral membrane. AP induced a concentration-dependent decrease in TER at 24 h (Fig. 6*b*) and an increase in HRP flux from 24 to 26 h (Fig. 6*c*). Thus, activation of PAR$_2$ at the basolateral membrane of T84 cells increases permeability.

PAR$_2$ Activation Induces Redistribution of TJ Proteins and F-actin—Alterations in the localization and expression of TJ proteins and perijunctional F-actin are associated with changes in paracellular permeability of epithelial cells. Therefore, we examined the effects of PAR$_2$ activation on localization of ZO-1, occludin, claudin-1, and F-actin in T84 cells by confocal microscopy. Optical sections in the x-y plane revealed that immunoreactive ZO-1 (Fig. 7*a*), occludin (Fig. 7*b*), and claudin-1 (Fig. 7*c*) were prominently localized to the perimeter at the apical pole in cells treated with RP (100 μM, 24 h). Projections in the z plane of stacks of optical sections confirmed the prominent localization of ZO-1, occludin, and claudin-1 in the apical region of the cell, consistent with the presence of these proteins in TJs. Lower levels of these proteins were detected in the basolateral membrane beneath the tight junctions and in the cytosol. Similar distributions were observed in cells treated with vehicle (not shown). In cells treated with AP (100 μM, 24 h), there was diminished intensity of staining for ZO-1 and occludin in the apical TJ region of cells. Both ZO-1 and occludin were more diffusely distributed, although it was not possible to discern whether there was diminished expression or redistribution of these proteins. The distribution of claudin-1 was not discernibly altered by exposure to AP. Staining was not observed when primary antibodies were replaced with isotype control antibodies, confirming specificity (Fig. 7*d*). F-actin was prominently detected in ring-like perijunctional structures in the perimeter of the apical pole of cells treated with RP (Fig. 7*e*) or vehicle

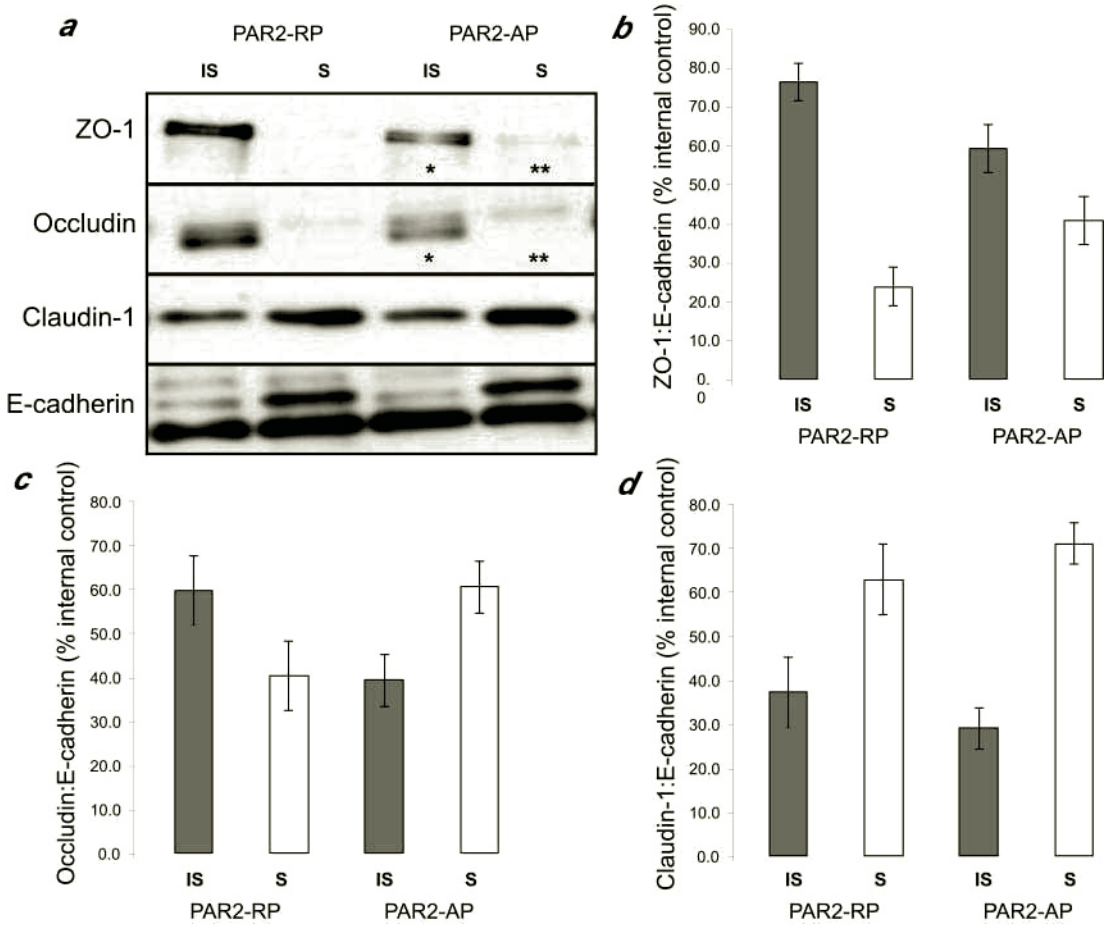

FIG. 8. **PAR_2-induced redistribution of TJ proteins detected by subcellular fractionation and Western blotting.** AP or RP (100 μM) were applied to T84 cells for 24 h. *a,* Western blots showing detection of ZO-1, occludin, claudin-1, and E-cadherin in detergent-insoluble (*IS*, junctional) and soluble (*S*, cytosolic) fractions by Western blotting. Note that AP induced loss of ZO-1 and occludin from the detergent-insoluble (*) and appearance in detergent-soluble (**) fractions, whereas there was no effect on claudin-1 or E-cadherin. Representative blot of four experiments is shown. *b–d,* densitometric analyses for ZO-1 (*b*), occludin (*c*), and claudin-1 (*d*) relative to E-cadherin in detergent-insoluble and -soluble fractions. Note the diminished levels of ZO-1 and occludin in the insoluble fractions and increased levels in the soluble fractions of cells treated with AP. $n = 4$ experiments.

(not shown). Exposure to AP resulted in a marked redistribution of F-actin from the perijunctional ring to particles within the cytosol (Fig. 7*e*).

We further investigated the redistribution of TJ proteins by detergent extraction of cells and Western blotting. In cells treated with vehicle (not shown) or RP (Fig. 8*a*), ZO-1 and occludin were mostly in the detergent-insoluble fraction (TJ-associated), with almost no detectable signal in the detergent-soluble fraction (cytoplasmic), whereas claudin-1 and E-cadherin were present in the TJs and the cytosol. AP resulted in appearance of ZO-1 and occludin in the cytosol and a loss from the TJs (Fig. 8*a*). AP did not affect the partitioning of claudin-1 or E-cadherin between the TJ and cytosol. Densitometric analysis, comparing ZO-1, occludin, and claudin-1 to E-cadherin signals confirmed these results (Fig. 8, *b–d*). The results are consistent with a PAR_2-induced increase in permeability.

Mast Cell Tryptase Increases Paracellular Permeability—To determine whether mediators from degranulated mast cells regulate permeability, we exposed the basolateral surface of T84 cells to supernatant from HMC1 treated with compound 48/80. The supernatant induced a decrease in TER that was detected within 1 h after stimulation and that was maximal after 4 h (30% reduction) (Fig. 9*a*). This effect was sustained and detected after 24 and 48 h from the initial stimulation. HMC1 supernatant also stimulated HRP flux, and after 24 h the HRP flux was elevated 4-fold in supernatant-treated cells (Fig. 9*b*). The tryptase inhibitor BABIM strongly inhibited the effects of supernatant on both TER and HRP flux, suggesting a prominent contribution of tryptase to the increased permeability (Fig. 9, *a* and *b*). However, BABIM did not affect TER or HRP flux in untreated T84 cells.

To examine paracrine regulation of colonocytes by mast cells, we co-cultured T84 cells on transwell filters with HMC1 cells in the basal compartment. The co-culture of HMC1 with T84 cells did not alter TER or HRP flux measured after 24 h (Fig. 9, *c* and *d*). However, addition of compound 48/80 to the basal compartment resulted in a 20% decline in TER and a 2-fold increase in HRP flux after 24 h, and BABIM strongly inhibited these effects. Compound 48/80 added to the basal compartment also increased tryptase activity in the medium (7.1 ± 2.3 nmol/min/10^6 cells after 24 h). However, compound 48/80 had no effect on TER or HRP flux of T84 cells culture in the absence of HMC1 cells. Thus, degranulated mast cells can signal to colonocytes in a paracrine manner by release of tryptase and probable activation of PAR_2 at the basolateral membrane to increase permeability.

βARRs and ERK1/2 Mediate PAR_2-induced Paracellular Permeability—Multiple signaling pathways regulate the assembly of TJs and the distribution of perijunctional F-actin to control permeability, including those that activate ERK1/2 (31). Because PAR_2 couples to activation of ERK1/2 (29, 30), we hypothesized that PAR_2 regulates permeability by an ERK1/2-

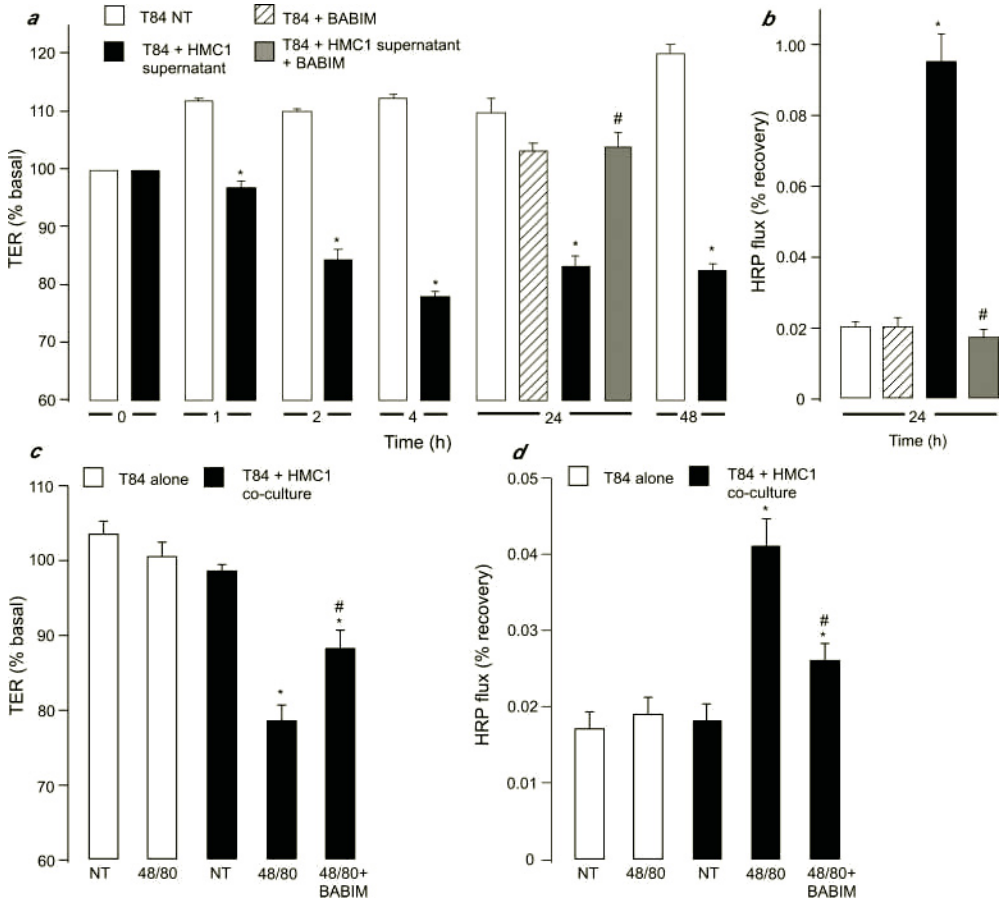

FIG. 9. **Effects of mast cell products on paracellular permeability.** *a* and *b,* T84 cells were cultured on transwell filters and treated with vehicle (*white bars*) or with supernatant from degranulated HMC1 cells diluted 1:1 in fresh medium and applied to the basal compartment (*black bars*). TER was measured from 0 to 48 h and is expressed as percentage of basal values at 0 min (*a*). HRP flux was determined from 24 to 26 h and is expressed as percentage of apically added HRP recovered into the basal compartment (*b*). Note that supernatant decreased TER and increased HRP flux; *, $p < 0.05$ compared with nontreated cells at each time point. Pretreatment of supernatant with the tryptase inhibitor BABIM (*gray bars*) significantly diminished the effect of supernatant on TER and HRP flux measured at 24 h; #, $p < 0.05$ compared with effects of supernatant without tryptase inhibitor. BABIM did not affect TER or HRP flux in T84 cells alone (*cross-hatched bars*). *c* and *d,* T84 cells were cultured on transwell filters alone (*white bars*) or with HMC1 cells cultured in the basal compartment for 24 h (*black bars*). TER was measured at 24 h (*c*), and HRP flux was determined from 24 to 26 h (*d*). In control experiments, compound 48/80 and BABIM had no effect on TER or HRP flux of T84 cells alone. Note that the addition of compound 48/80 significantly decreased TER and increased HRP flux in T84 cells co-cultured with HMC1 cells; *, $p < 0.05$ to nontreated (*NT*) co-cultures. BABIM significantly inhibited the effects of compound 48/80; #, $p < 0.05$ to compound 48/80-treated co-cultured cells. Quadruplicate observations in $n = 4$ experiments.

mediated mechanism. AP (100 μM) induced a rapid phosphorylation and thus activation of ERK1/2 in T84 cells that was maximal after 10–15 min, assessed by Western blotting (Fig. 10*a*). The MEK1/2 inhibitor UO126 (10 μM) prevented AP-induced phosphorylation of ERK1/2 (not shown). UO126 also strongly inhibited the AP-induced decrease in TER observed after 24 h (Fig. 10*b*) and prevented AP-stimulated redistribution of perijunctional F-actin (Fig. 10*c*). Together, these results suggest that ERK1/2 mediates AP-induced increases in permeability.

In enterocytes, βARRs recruit Raf-1, MEK1/2, and ERK1/2 to activated PAR$_2$ in endosomes (29). This mechanism retains activated ERK1/2 in the cytosol where they may regulate cytosolic targets such as cytoskeletal and junctional proteins (30). To determine the importance of this pathway in PAR$_2$-induced alterations in permeability, we down-regulated βARRs using siRNA. Transcripts corresponding to the predicted size of βARR1 (498 bp) and βARR2 (381 bp) were amplified from T84 cells and identified by sequencing, suggesting that T84 cells express both isoforms of βARRs (Fig. 11*a*). Because PAR$_2$ can interact with βARR1 and βARR2 (37), we used siRNA to down-regulate both isoforms in T84 cells. siRNA to βARR1 and -2 down-regulated both βARRs by >50% within 3–4 days as determined by Western blotting (Fig. 11*b*) and strongly reduced mRNA levels as determined by RT-PCR (not shown). Control siRNA had no effect on expression of βARRs. Down-regulation of βARR1 and -2 resulted in a >2-fold inhibition of AP-induced activation of ERK1/2 (Fig. 11*c*).

To determine the importance of βARR-mediated activation of ERK1/2 to PAR$_2$-induced changes in permeability, we examined the effects of AP on TER and HRP flux. Oligofectamine or control siRNA had no effect on AP-induced inhibition of TER or stimulation of HRP flux (Fig. 12, *a* and *b*). However, siRNA to βARR1 and -2 strongly inhibited the AP-induced decrease in TER and increase in HRP flux at 24 h (Fig. 12, *a* and *b*). Thus, βARRs are required for PAR$_2$-induced activation of ERK1/2 and increased permeability.

DISCUSSION

Our results show that mast cells release tryptase, which activates PAR$_2$ on the basolateral membrane of colonocytes to trigger redistribution of ZO-1, occludin, and F-actin by a βARR- and ERK1/2-dependent process. This mechanism increases paracellular permeability to macromolecules and may explain the critical role of mast cells in the increased permeability of the intestine during stress and inflammation (5, 6, 9–11). In

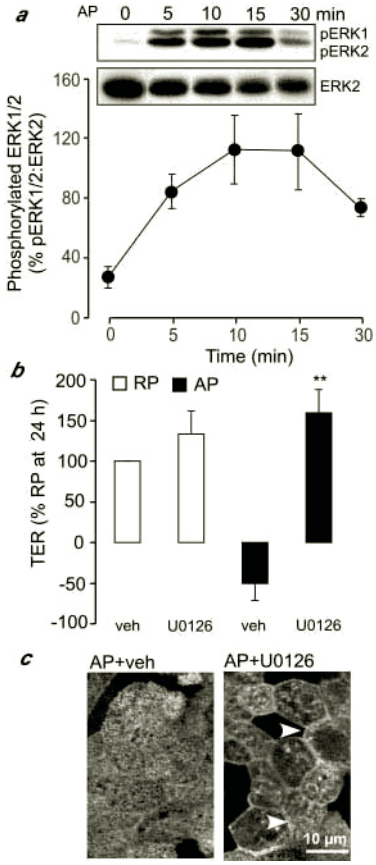

FIG. 10. **ERK1/2-mediated changes in paracellular permeability.** *a,* effects of AP (100 μM) on the expression of phosphorylated pERK1/2 and total ERK2 in T84 cells. The *insets* show representative blots, and the *graph* shows pERK1/2 expressed as a percentage of the densitometric ratios of pERK1/2, total ERK2 (n = 4 experiments). *b,* effects of the MEK1/2 inhibitor UO126 or vehicle (*veh*) on TER measured in T84 cells at 24 h after basolateral application of AP or RP (100 μM). TER is expressed as a percentage of the RP response in vehicle-treated cells (n = 4 experiments). Note that UO126 prevented the AP-induced decrease in TER. *, $p < 0.05$ to vehicle. *c,* effects of UO126 or vehicle on the localization of F-actin determined with Texas Red phalloidin in T84 cells 24 h after basolateral application of AP (100 μM). Note that UO126 prevented the redistribution of the perijunctional F-actin (representative image of $n > 4$ experiments).

this manner, proteases and PAR_2 play a critical role in disrupting the intestinal barrier and promoting the ingress of macromolecules and bacteria that cause inflammation and infection (26–28).

Mast Cell Proteases and PAR$_2$ Regulate Paracellular Permeability—Colonocytes expressed PAR_2 mRNA, and both trypsin- and PAR_2-specific AP increased $[Ca^{2+}]_i$, confirming expression of functional receptors. The elevation in $[Ca^{2+}]_i$ to PAR_2 agonists was biphasic, comprising an initial increase followed by a more sustained plateau, both of which were diminished by removal of extracellular Ca^{2+} ions. We have reported previously a similar biphasic response in PAR_2-transfected cells and in enterocytes and tumor cell lines that naturally express this receptor (38, 39). However, the plateau response in transfected epithelial cells and enterocytes is more strongly inhibited by removal of extracellular Ca^{2+} ions and is thus more dependent on Ca^{2+} influx that in colonocytes. These differences may reflect disparate mechanisms by which PAR_2 regulates Ca^{2+} channels in the plasma membrane that are responsible for the influx of Ca^{2+} ions. The potency with which trypsin increased $[Ca^{2+}]_i$ in colonocytes was ~1,000-fold greater than the potency of AP. Agonists had similar potencies in both NCM460 and T84 cells that are comparable with potencies reported for these agonists in transfected cells, enterocytes, and tumor cell lines (38). Moreover, preincubation of cells with trypsin strongly desensitized responses to AP, as we have observed previously in transfected cells and enterocytes (39). Together, these results suggest that trypsin and AP increased $[Ca^{2+}]_i$ in colonocytes by activating PAR_2. However, we cannot exclude the possibility that trypsin also activates other receptors in these cells, such as PAR_4 (19). In support of our results, other intestinal epithelial cell lines also express PAR_2 and respond to trypsin and AP (20, 29, 40).

Supernatants from two mast cell lines degranulated by cross-linking IgE receptors or by treatment with compound 48/80 triggered increased $[Ca^{2+}]_i$ in NCM460 and T84 cells. The supernatants contained enzymatic activity that was suppressed by two tryptase inhibitors, but unaffected by a trypsin-selective inhibitor, and is thus likely to be tryptase. Moreover, a tryptase inhibitor reduced the effects of the supernatant on the $[Ca^{2+}]_i$ by ~50%. Thus, tryptase plays a major role in mediating the effects of mast cell supernatant on $[Ca^{2+}]_i$ in colonocytes. Other factors released by degranulated mast cells, such histamine, serotonin, and prostaglandins, may also contribute to the activity of the supernatant that was unaffected by the tryptase inhibitor. Preincubation of colonocytes with mast cell supernatant reduced the responses to AP by ~50%, suggesting that tryptase in the supernatant cleaved PAR_2, resulting in homologous desensitization of this receptor. In support of these results, we have reported previously that supernatants from degranulated mast cells increase $[Ca^{2+}]_i$ in colonic myocytes and ileal myenteric neurons by a tryptase-dependent mechanism and desensitize responses of these cells to PAR_2-selective AP (22, 41). However, the observation that supernatants desensitized responses to AP does not unequivocally prove activation of PAR_2, because certain mast cell products may activate other receptors and signaling pathways that result in heterologous desensitization of PAR_2.

By studying monolayers of T84 cells that form TJs and maintain a high TER, we determined the effects of selectively activating PAR_2 at the basolateral or apical membranes on permeability. When applied to the basolateral membrane, AP and trypsin decreased TER and increased transepithelial flux of macromolecules from the apical to the basolateral compartments, consistent with an increased permeability. The magnitude of these effects is similar to what we have observed with cytokines such as interleukin 4 and atopic serum (42). The PAR_2 agonists were more effective when applied basolaterally than apically, which is consistent with reports that serosally applied PAR_2 agonists promote electrolyte secretion from intestinal tissue, whereas agonists applied to the mucosal surface are less effective (43–45). However, PAR_2 agonists increase permeability when injected into the colonic lumen of rats and mice (26–28), and physiological concentrations of trypsin in the intestinal lumen can signal to enterocytes by cleaving apical PAR_2 (20). Thus, activation of PAR_2 at the basolateral and apical membranes of colonocytes may increase epithelial permeability.

Supernatants from degranulated mast cells, when applied to the basolateral membranes of colonocytes, decreased TER and increased macromolecular flux, indicative of increased epithelial permeability. Furthermore, when mast cells were co-cultured with colonocytes, degranulation of mast cells resulted in a marked increase in permeability of colonocytes. Tryptase inhibitors strongly reduced the effects of mast cell supernatant and of mast cell degranulation on the permeability of colonocytes. Thus, upon degranulation, mast cells increase paracellular permeability of colonocytes by a tryptase-dependent mechanism that is probably due to activation of PAR_2 on the

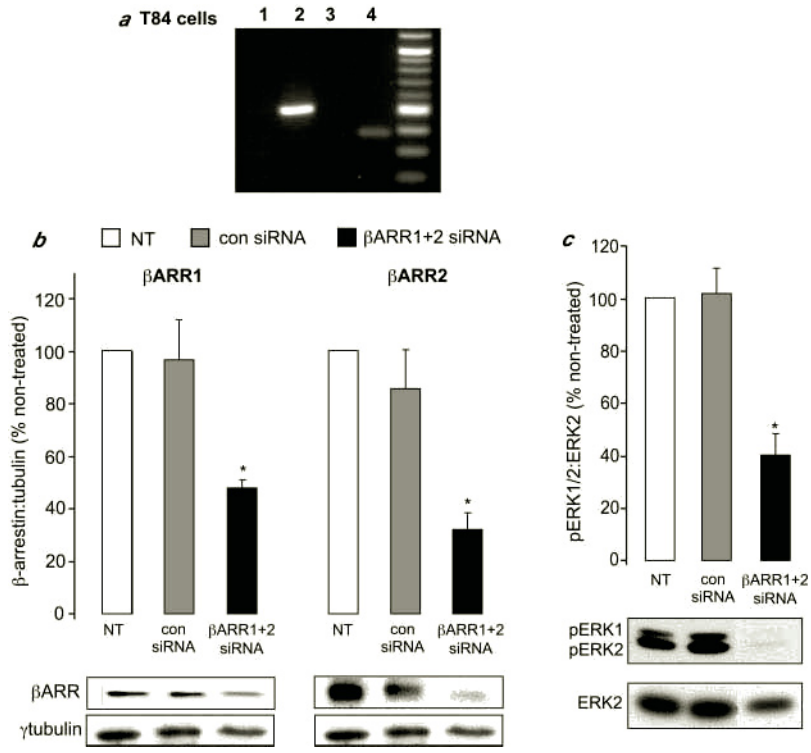

FIG. 11. **Down-regulation of βARR using siRNA.** *a,* amplification of βARR1 (*lane 2*) and βARR2 (*lane 4*) in T84 cells by RT-PCR. *Lanes 1* and *3* are controls (no RT). The products were identified by sequencing. *b,* effects of no treatment (*NT*), control siRNA (*con*), or siRNA to βARR1 and -2 on expression levels of βARR1 (*left panel*) and βARR2 (*right panel*) in T84 cells determined by Western blotting. The *insets* show representative blots, and the *graphs* are densitometric ratios of βARR, tubulin signals expressed as percentage of the ratios in nontreated cells ($n = 3$ experiments). *, $p < 0.05$ to control siRNA. *c,* effects of no treatment (*NT*), control siRNA (*con*), or siRNA to βARR1 and -2 on AP (100 μM, 10–15 min)-stimulated levels of pERK1/2 in T84 cells determined by Western blotting. The *insets* show representative blots, and the *graphs* are densitometric ratios of pERK1/2:total ERK2 expressed as percentage of the ratios in nontreated cells ($n = 4$ experiments). *, $p < 0.05$ to control siRNA.

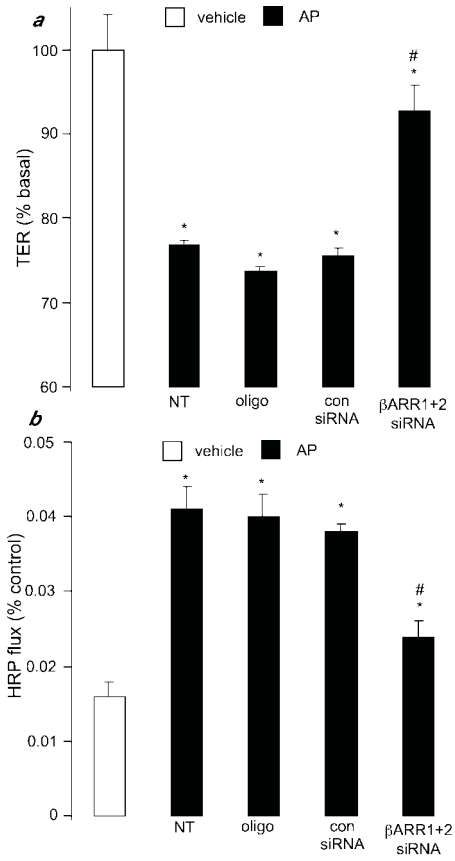

FIG. 12. **βARR-mediated changes in paracellular permeability.** T84 cells were not-treated (*NT*), treated with Oligofectamine alone (*oligo*), or transfected with control siRNA (*con*) or siRNA to βARR1 and -2. After 3 days, AP (100 μM) or vehicle was applied to the basolateral membrane, and TER was measured at 24 h (*a*) and HRP flux from 24 to 26 h (*b*). Note that siRNA to βARR1 and -2 strongly inhibited the effects of AP on TER and HRP flux but that Oligofectamine and control siRNA had no effect. *, $p < 0.05$ to vehicle-treated cells; #, $p < 0.05$ to control siRNA. Quadruplicate observations in $n = 4$ experiments.

basolateral membrane. We propose that this mechanism accounts for the observation that the increased permeability of the intestine during chronic stress, allergic inflammation, parasitic infection, and chemically induced inflammation is reduced in mast cell-deficient animals and by mast cell stabilizers (5, 6, 9–11). Experiments with tryptase inhibitors and PAR_2-deficient animals are underway to investigate directly this hypothesis.

Tryptase inhibitors reduced but did not abolish the effects of mast cell supernatant on $[Ca^{2+}]_i$ and permeability of colonocytes, suggesting that mast cell mediators other than tryptase may also regulate permeability. For example, tumor necrosis factor α increases the permeability of intestinal epithelial cells, which may contribute to the loss of the epithelial barrier in inflammatory bowel disease (46). Mast cell supernatant desensitized AP-induced Ca^{2+} signaling in colonocytes and mimicked the effects of AP on permeability. Thus, PAR_2 probably mediates the effects of mast cell proteases on permeability. However, mast cell proteases may regulate permeability by additional mechanisms, possibly by degrading junctional proteins, as suggested for mouse mast cell protease-1 (6).

In addition to tryptase, there are elevated levels of trypsins and activation of coagulation proteases in the inflamed intestine, which may also regulate permeability by cleaving PARs (15–18). Although the precise form of trypsin that is up-regulated in the inflamed intestine is unknown, one possibility is trypsin IV, which is prominently expressed in the human colon and activates PAR_2 (24). These proteases may regulate permeability by cleaving PAR_2 or other PARs, such as PAR_1 and PAR_4, which are also expressed in the colon (47, 48). Activation of PAR_1 increases permeability by inducing apoptosis of epithelial cells (47).

Mechanisms of PAR_2 Regulation of Paracellular Permeability—PAR_2 agonists induced redistribution of ZO-1 and occludin from TJs and caused translocation of perijunctional F-actin to the cytosol, as determined by confocal microscopy and subcellular fractionation. We have observed similar effects of PAR_2 agonists on the localization of ZO-1 in enterocytes,[2] and others

have reported (28) that AP induces redistribution of ZO-1 from tight junctions to the cytoplasm of SCBN cells in culture. A similar redistribution of TJ proteins and perijunctional actin is observed in the inflamed intestine (2–6) and in epithelial cells treated with other agents that increase permeability (7, 8). Together, they would be expected to increase paracellular permeability.

Several signaling pathways may account for PAR_2-mediated alterations in paracellular permeability, including calmodulin-mediated activation of myosin light chain kinase and the resultant phosphorylation of myosin light chain, which occurs in the colon of mice treated with PAR_2-AP (28). The observation that a MEK1/2 inhibitor prevented the effects of AP on TER and F-actin redistribution suggests that activation of ERK1/2 is required for PAR_2-induced increases in permeability. Supporting this possibility, PAR_2 activates ERK1/2 in colonocytes and enterocytes (29, 40), and MEK1/2 inhibition suppresses AP-induced formation of stress fibers in fibroblasts (30). ERK1/2 also regulate permeability in other epithelial cell lines possibly through phosphorylation of cytoskeletal or TJ proteins (31). To regulate cytosolic or cytoskeletal targets, activated ERK1/2 must be retained in the cytosol rather than translocating to the nucleus. Many pathways may couple activated PAR_2 to ERK1/2 in intestinal epithelial cells, including protein kinase C (29) and transactivation of the epidermal growth factor receptor (40). However, these pathways lead to nuclear translocation of ERK1/2 and stimulation of proliferation, rather than regulation of cytosolic targets. We have previously reported that βARRs are scaffolds that recruit Raf-1, MEK1/2, and ERK1/2 to activated PAR_2 in endosomes, thereby preventing the nuclear trafficking of these kinases (29). We found that down-regulation of βARRs strongly inhibited AP-induced activation of ERK1/2 and prevented increased permeability and reorganization of F-actin in response to AP. These results suggest that cytosolically retained ERK1/2 regulates the cytoskeleton to control the permeability of TJs.

Proteases that are released and generated during intestinal inflammation may regulate paracellular permeability by directly activating PAR_2 on epithelial cells or by indirect mechanisms that are secondary to PAR_2-induced intestinal inflammation. Our observations on colonic epithelial cells in culture indicate that PAR_2 agonists can directly regulate paracellular permeability, and our observations support previous studies (28) showing direct effects of PAR_2 agonists on the permeability of cultured enterocytes. Furthermore, the intracolonic injection in mice of low doses of PAR_2 AP, which do not cause detectable inflammation, increases permeability, presumably due to a direct action on colonocytes (28). However, at higher doses PAR_2 agonists also trigger intestinal inflammation by mechanisms that depend on the release of proinflammatory peptides substance P and calcitonin gene-related peptide from sensory nerves and on the generation of nitric oxide (27, 49). This PAR_2-induced inflammation results in elevated tissue levels of tumor necrosis factor α and interferon γ (28), which can in turn increase paracellular permeability (46, 50).

In summary, upon degranulation mast cells release tryptase, which cleaves PAR_2 on the basolateral membrane of colonocytes, thereby activating ERK1/2. βARRs retain ERK1/2 in the cytosol, where they induce redistribution of TJ proteins and perijunctional F-actin, to increase paracellular permeability. Because TJs between colonocytes are an essential component of the barrier to the ingress of luminal bacteria and macromolecules, this mechanism may be of critical importance to the control of inflammation and infection in the intestine. Additional experiments with tryptase inhibitors and PAR_2-deficient animals are required to define the importance of this mechanism in inflammation and stress-induced alterations in permeability of the colonic mucosa.

Acknowledgments—We thank Brian Wong and Alexander Rossi (Rigel Pharmaceuticals) for providing the CHMC.

REFERENCES

1. Schneeberger, E. E., and Lynch, R. D. (2004) *Am. J. Physiol.* **286,** C1213–C1228
2. May, G. R., Sutherland, L. R., and Meddings, J. B. (1993) *Gastroenterology* **104,** 1627–1632
3. Schmitz, H., Barmeyer, C., Fromm, M., Runkel, N., Foss, H. D., Bentzel, C. J., Riecken, E. O., and Schulzke, J. D. (1999) *Gastroenterology* **116,** 301–309
4. Gassler, N., Rohr, C., Schneider, A., Kartenbeck, J., Bach, A., Obermuller, N., Otto, H. F., and Autschbach, F. (2001) *Am. J. Physiol.* **281,** G216–G228
5. Stein, J., Ries, J., and Barrett, K. E. (1998) *Am. J. Physiol.* **274,** G203–G209
6. McDermott, J. R., Bartram, R. E., Knight, P. A., Miller, H. R., Garrod, D. R., and Grencis, R. K. (2003) *Proc. Natl. Acad. Sci. U. S. A.* **100,** 7761–7766
7. Chen, M. L., Pothoulakis, C., and LaMont, J. T. (2002) *J. Biol. Chem.* **277,** 4247–4254
8. Bruewer, M., Luegering, A., Kucharzik, T., Parkos, C. A., Madara, J. L., Hopkins, A. M., and Nusrat, A. (2003) *J. Immunol.* **171,** 6164–6172
9. Santos, J., Yang, P. C., Soderholm, J. D., Benjamin, M., and Perdue, M. H. (2001) *Gut* **48,** 630–636
10. Soderholm, J. D., Yang, P. C., Ceponis, P., Vohra, A., Riddell, R., Sherman, P. M., and Perdue, M. H. (2002) *Gastroenterology* **123,** 1099–1108
11. Yang, P. C., Berin, M. C., and Perdue, M. H. (1999) *J. Immunol.* **163,** 2769–2776
12. Miller, H. R., and Pemberton, A. D. (2002) *Immunology* **105,** 375–390
13. Scudamore, C. L., Thornton, E. M., McMillan, L., Newlands, G. F., and Miller, H. R. (1995) *J. Exp. Med.* **182,** 1871–1881
14. Santos, J., Bayarri, C., Saperas, E., Nogueiras, C., Antolin, M., Mourelle, M., Cadahia, A., and Malagelada, J. R. (1999) *Gut* **45,** 553–558
15. Playford, R. J., Hanby, A. M., Patel, K., and Calam, J. (1995) *Am. J. Pathol.* **146,** 310–316
16. Bustos, D., Negri, G., De Paula, J. A., Di Carlo, M., Yapur, V., Facente, A., and De Paula, A. (1998) *Medicina* (*B. Aires*) **58,** 262–264
17. Tarlton, J. F., Whiting, C. V., Tunmore, D., Bregenholt, S., Reimann, J., Claesson, M. H., and Bland, P. W. (2000) *Am. J. Pathol.* **157,** 1927–1935
18. Kjeldsen, J., Lassen, J. F., Brandslund, I., and Schaffalitzky de Muckadell, O. B. (1998) *Scand. J. Gastroenterol.* **33,** 637–643
19. Ossovskaya, V. S., and Bunnett, N. W. (2004) *Physiol. Rev.* **84,** 579–621
20. Kong, W., McConalogue, K., Khitin, L. M., Hollenberg, M. D., Payan, D. G., Bohm, S. K., and Bunnett, N. W. (1997) *Proc. Natl. Acad. Sci. U. S. A.* **94,** 8884–8889
21. Molino, M., Barnathan, E. S., Numerof, R., Clark, J., Dreyer, M., Cumashi, A., Hoxie, J. A., Schechter, N., Woolkalis, M., and Brass, L. F. (1997) *J. Biol. Chem.* **272,** 4043–4049
22. Corvera, C. U., Dery, O., McConalogue, K., Bohm, S. K., Khitin, L. M., Caughey, G. H., Payan, D. G., and Bunnett, N. W. (1997) *J. Clin. Investig.* **100,** 1383–1393
23. Nystedt, S., Emilsson, K., Wahlestedt, C., and Sundelin, J. (1994) *Proc. Natl. Acad. Sci. U. S. A.* **91,** 9208–9212
24. Cottrell, G. S., Amadesi, S., Grady, E. F., and Bunnett, N. W. (2004) *J. Biol. Chem.* **279,** 13532–13539
25. Camerer, E., Huang, W., and Coughlin, S. R. (2000) *Proc. Natl. Acad. Sci. U. S. A.* **97,** 5255–5260
26. Cenac, N., Coelho, A. M., Nguyen, C., Compton, S., Andrade-Gordon, P., MacNaughton, W. K., Wallace, J. L., Hollenberg, M. D., Bunnett, N. W., Garcia-Villar, R., Bueno, L., and Vergnolle, N. (2002) *Am. J. Pathol.* **161,** 1903–1915
27. Cenac, N., Garcia-Villar, R., Ferrier, L., Larauche, M., Vergnolle, N., Bunnett, N. W., Coelho, A. M., Fioramonti, J., and Bueno, L. (2003) *J. Immunol.* **170,** 4296–4300
28. Cenac, N., Chin, A. C., Garcia-Villar, R., Salvador-Cartier, C., Ferrier, L., Vergnolle, N., Buret, A. G., Fioramonti, J., and Bueno, L. (2004) *J. Physiol.* (*Lond.*) **558,** 913–925
29. DeFea, K. A., Zalevsky, J., Thoma, M. S., Dery, O., Mullins, R. D., and Bunnett, N. W. (2000) *J. Cell Biol.* **148,** 1267–1281
30. Ge, L., Ly, Y., Hollenberg, M., and DeFea, K. (2003) *J. Biol. Chem.* **278,** 34418–34426
31. Wang, Y., Zhang, J., Yi, X. J., and Yu, F. S. (2004) *Exp. Eye Res.* **78,** 125–136
32. Steinhoff, M., Vergnolle, N., Young, S. H., Tognetto, M., Amadesi, S., Ennes, H. S., Trevisani, M., Hollenberg, M. D., Wallace, J. L., Caughey, G. H., Mitchell, S. E., Williams, L. M., Geppetti, P., Mayer, E. A., and Bunnett, N. W. (2000) *Nat. Med.* **6,** 151–158
33. Caughey, G. H., Raymond, W. W., Bacci, E., Lombardy, R. J., and Tidwell, R. R. (1993) *J. Pharmacol. Exp. Ther.* **264,** 676–682
34. Costanzo, M. J., Yabut, S. C., Almond, H. R., Jr., Andrade-Gordon, P., Corcoran, T. W., De Garavilla, L., Kauffman, J. A., Abraham, W. M., Recacha, R., Chattopadhyay, D., and Maryanoff, B. E. (2003) *J. Med. Chem.* **46,** 3865–3876
35. Moyer, M. P., Manzano, L. A., Merriman, R. L., Stauffer, J. S., and Tanzer, L. R. (1996) *In Vitro Cell Dev. Biol. Anim.* **32,** 315–317
36. Butterfield, J., Weiler, D., Hunt, L., Wynn, S., and Roche, P. (1990) *J. Leukocyte Biol.* **47,** 409–419
37. Dery, O., Thoma, M. S., Wong, H., Grady, E. F., and Bunnett, N. W. (1999) *J. Biol. Chem.* **274,** 18524–18535
38. Bohm, S. K., Kong, W., Bromme, D., Smeekens, S. P., Anderson, D. C., Connolly, A., Kahn, M., Nelken, N. A., Coughlin, S. R., Payan, D. G., and

Bunnett, N. W. (1996) *Biochem. J.* **314,** 1009–1016
39. Bohm, S. K., Khitin, L. M., Grady, E. F., Aponte, G., Payan, D. G., and Bunnett, N. W. (1996) *J. Biol. Chem.* **271,** 22003–22016
40. Darmoul, D., Gratio, V., Devaud, H., and Laburthe, M. (2004) *J. Biol. Chem.* **279,** 20927–20934
41. Corvera, C. U., Dery, O., McConalogue, K., Gamp, P., Thoma, M., Al-Ani, B., Caughey, G. H., Hollenberg, M. D., and Bunnett, N. W. (1999) *J. Physiol.* (*Lond.*) **517,** 741–756
42. Berin, M. C., Yang, P. C., Ciok, L., Waserman, S., and Perdue, M. H. (1999) *Am. J. Physiol.* **276,** C1046–C1052
43. Vergnolle, N., Macnaughton, W. K., Al-Ani, B., Saifeddine, M., Wallace, J. L., and Hollenberg, M. D. (1998) *Proc. Natl. Acad. Sci. U. S. A.* **95,** 7766–7771
44. Green, B. T., Bunnett, N. W., Kulkarni-Narla, A., Steinhoff, M., and Brown, D. R. (2000) *J. Pharmacol. Exp. Ther.* **295,** 410–416
45. Cuffe, J. E., Bertog, M., Velazquez-Rocha, S., Dery, O., Bunnett, N., and Korbmacher, C. (2002) *J. Physiol.* (*Lond.*) **539,** 209–222
46. Ma, T. Y., Iwamoto, G. K., Hoa, N. T., Akotia, V., Pedram, A., Boivin, M. A., and Said, H. M. (2004) *Am. J. Physiol.* **286,** G367–G376
47. Chin, A. C., Vergnolle, N., MacNaughton, W. K., Wallace, J. L., Hollenberg, M. D., and Buret, A. G. (2003) *Proc. Natl. Acad. Sci. U. S. A.* **100,** 11104–11109
48. Mule, F., Pizzuti, R., Capparelli, A., and Vergnolle, N. (2004) *Gut* **53,** 229–234
49. Nguyen, C., Coelho, A. M., Grady, E., Compton, S. J., Wallace, J. L., Hollenberg, M. D., Cenac, N., Garcia-Villar, R., Bueno, L., Steinhoff, M., Bunnett, N. W., and Vergnolle, N. (2003) *Can. J. Physiol. Pharmacol.* **81,** 920–927
50. Youakim, A., and Ahdieh, M. (1999) *Am. J. Physiol.* **276,** G1279–G1288